Temperature distribution of a Fast-Field Cycling Nuclear Magnetic Resonance relaxometer's electromagnet with reduced volume

P. Videira[1], P. Sebastião[1], A. Roque[2,4], D. M. Sousa[3,4], A. Fernandes[2], E. Margato[4,5]

[1]Department of Physics & CeFEMA, Instituto Superior Técnico, Universidade de Lisboa
Lisbon, Portugal, Av. Rovisco Pais, 1 – 1049-001 Lisboa, Portugal, Phone/Fax number: +351 218417310,
pedrovideira@live.com.pt, pedro.jose.sebastiao@tecnico.ulisboa.pt

[2]Department of Electrical Engineering
ESTSetúbal/Instituto Politécnico de Setúbal
Campus of IPS, Estefanilha, 2914-761 Setúbal, Portugal
Phone/Fax: +351 265790000; **antonio.roque@estsetubal.ips.pt**

[3]DEEC AC-Energia, Instituto Superior Técnico, Universidade de Lisboa
Av. Rovisco Pais, 1 – 1049-001 Lisboa, Portugal, Phone/Fax number: +351 218417429/+351 218417167,
duarte.sousa@tecnico.ulisboa.pt

[4]INESC-ID
Av. Alves Redol 9, 1000-029 Lisboa, Portugal
Phone/Fax: +351 213100300/ +351 213100235 Lisboa, Portugal

[5]CEI, ISEL-Instituo Superior de Engenharia de Lisboa, Instituto Politécnico de Lisboa, and INESC-ID, Av. Rua
Conselheiro Emídio Navarro 1959-007 Lisboa, Portugal, Phone/Fax: +35121 8417429/+351218417167,
efmargato@isel.ipl.pt

Abstract. The temperature distribution of a Fast Field Cycling (FFC) Nuclear Magnetic Resonance (NMR) electromagnet plays an important role in the operation of this type of apparatus. The designed electromagnet presents a reduced volume and is iron and copper based, fulfilling the technical requirements for the magnetic field. With this solution, it is possible to increase the overall performance in comparison with former similar FFC relaxometers. Electromagnet's simulation results evaluating the temperature distribution, heating effects and cooling requirements are presented.

Key words. Temperature distribution, Electromagnet, Relaxometer, Fast Field Cycling.

1. Introduction

Nuclear magnetic resonance is a physical phenomenon which occurs when the nuclei of certain atoms are immersed in a static magnetic field and exposed to a second oscillating magnetic field. Some nuclei experience this phenomenon, and others do not, dependent upon whether they possess a property called spin. All isotopes that contain an odd number of protons and/or neutrons have a nonzero spin, making them susceptible to magnetic stimulus and therefore suitable for NMR studies.

In nuclear magnetic resonance, nuclear spins interact with the applied external static magnetic field by aligning with it. The average alignment reflects a precession around the external magnetic field due to their nuclear magnetic moment, $\vec{\mu}_i$. This precession has a specific frequency, the so called Larmor frequency, which depends on the applied field and nuclear species:

$$\vartheta_L = \frac{\gamma}{2\pi} B_0 \tag{1}$$

γ stands for the gyromagnetic ratio of the nucleus.

The alignment of the net magnetization with the external magnetic field can be disturbed by radio frequency pulses. After a perturbation the spins realign again with the external magnetic in a process called relaxation.

The set of the Bloch equations describes this phenomenon assuming a static magnetic field $\vec{B} = B_0 \vec{e}_z$ and magnetization $\vec{M} = M_0 \vec{e}_z$ [1-3].

$$
\begin{cases}
\dfrac{dM_x(t)}{dt} = \left[\vec{M} \times \gamma\vec{B}\right]_x - \dfrac{M_z(t) - M_0}{T_1} \\[2mm]
\dfrac{dM_y(t)}{dt} = \left[\vec{M} \times \gamma\vec{B}\right]_y - \dfrac{M_x(t)}{T_2} \\[2mm]
\dfrac{dM_z}{dt} = \left[\vec{M} \times \gamma\vec{B}\right]_z - \dfrac{M_y(t)}{T_2}
\end{cases}
\tag{2}
$$

The time constants T_1 and T_2 related to the realignment of nuclei magnetizations with the external field are called relaxation rates and nuclear magnetic resonance

experiments are precisely used to acquire frequency dependence of relaxation rates.

The spin-lattice relaxation time, T_1 is the time constant for the physical processes responsible for the relaxation of the components of the nuclear spin magnetization vector $\vec{M}$ parallel to the external magnetic field, $\overrightarrow{B_0}$ (z component, also named longitudinal component). Values of T_1 range from milliseconds to several seconds [4-6].

Spin-spin relaxation time, T_2 is at its most fundamental level the evolution time towards the decoherence of the transverse nuclear spin magnetization. Fluctuations of the local magnetic field lead to random variations in the instantaneous NMR precession frequency of different spins. As a result, the initial phase coherence of the nuclear spins is lost, until eventually the phases are disordered and there is no net xy magnetization.

The Fast Field Cycling (FFC) equipment proposed in this document, will only measure spin-lattice relaxation time, T_1.

In a typical field-cycling NMR relaxometry experiment the sample is initially placed on a magnetic field, as high as possible, where it is polarized. This initial magnetic field is called polarization field, B_{oP}. Typically, it is oriented with the z axis, and forces the nuclear spin magnetization to be along, $\vec{M} = M_0 \vec{e}_z$. Following this, the magnetic field is switched down to a lower value B_{oE}. In this new applied field, evolution field, the magnetization evolves to a new equilibrium, $M(B_E)$.

The final stage of the cycle, is the detection stage. The magnetic field is again increased to a high value, B_{oD}, with sufficient homogeneity to allow NMR signal detection, along with a π/2 RF pulse, rotating the magnetization to the *xy* plane. A recycle delay follows, where thermal equilibrium and polarization is reset, in order to begin the next cycle.

Several cycles will occur with different parameters in order to observe the behavior of the spin system. As the sample has to experience different intensities of Bo field, there are two methods to achieve this. Mechanically moving the sample between positions of different magnetic fields, or to change the electrical current applied to the magnet in order to vary the intensity of the field. Despite the difficulties of achieving a short steady transition (3-100ms) between fields, electronically switched field cycling is the only known alternative for measuring the shortest relaxation times.

FFC magnets are designed and optimized using simulation tools for their thermal and electromagnetic behavior. These computational tools are based on the finite element method and constitute an important step towards the construction of the magnet.

In this work, the computational applications aimed at the thermal behavior of a magnet with a parallelepiped structure, from which the need for cooling by forced convection is easily understood.

In this context, and using the analysis carried out, it was possible to move towards an FFC magnet with dimensions smaller than those developed in previous generations. This advance aim to allow the use of the FFC NMR technique in industrial development laboratories. In addition, efficient cooling of the magnet allows to increase the magnetic field and, thus, to allow the use of the technique to study the molecular dynamics of more samples.

2. Heating Effects

The core component of the FFC equipment is the electromagnet. The electromagnet geometry will be based on the previous equipment developed in IST [7-10]. This geometry is composed by transformer E-shaped plates. These plates are piled together in order to avoid induced currents. The electromagnet consists of two symmetrical E shape plates brought together with a slight cut on each of the middle feet where the sample will be accommodated. The electromagnet's height is equal to the middle feet length in order to accommodate squared coils. In Fig. 1 the electromagnet can be observed.

The desired parameters of the electromagnet were designed and compiled. Two additional coils were added to serve the purpose of auxiliary coils, which compensate permanent magnetizations of the electromagnet and the earth magnetic field. These coils are composed of 430 turns each with a copper wire of 0:25 mm diameter.
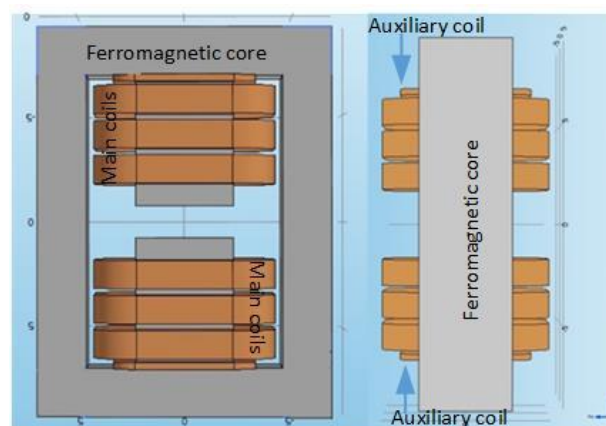

Fig. 1. Electromagnet structure.

To evaluate the total resistance of the coils, the experimental resistance is $9.6 \pm 0.1\ \Omega$ compared to the 9.3 Ω theoretically calculated.

The inductance of the coils come as an important parameter to measure given its relation with the current variations necessary for field cycling. A direct measurement of the inductance was performed for all the six coils with an Inductance-meter which revealed: $L = 544.5 \pm 0:1$ mH. The auxiliary coils both measured an inductance of $L = 134.2 \pm 0.1$ mH.

The magnetic field creation leads to heating effects. This heating effects are caused by Joule losses in the coils and need to be assessed in order to avoid damage or melting of the components of the system. So one may evaluate this effect and understand the requirements of the cooling system by simulation. The Joule heating dissipation of then coils in the chosen case of an applied current of 3 A to the coils is 84 W requiring a fan as shown in Fig. 2.
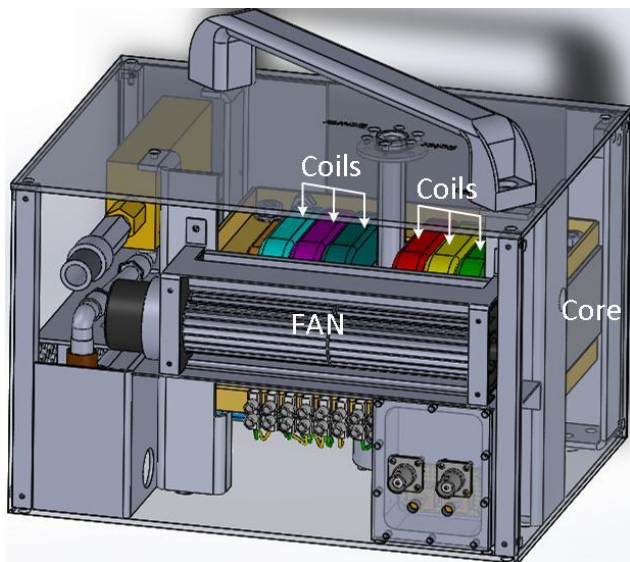
Fig. 2. Magnet enclosure with all parts.

The coils will typically only be under such current in the polarization and detection phase of a fast field cycle a dissipation equivalent of constant 3 A happens when measuring the spin lattice relaxation time for a field of 0:33 T. By considering this case we are also able to overestimate the cooling requirements allowing to design a reliable cooling system. A stationary study will be performed to understand the equilibrium of the system when a 3 A current is applied over large ranges of time, by simulation based on the Finite Element Method [11-18].

The defined problem for the Joule Heating effect can be summed up to: The electromagnet geometry with six coils dissipate a total of 84 W surrounded by air at a temperature of 20 ºC. The initial temperature of the system is 20 ºC , the heat coefficient between the air and the geometry is 5 W=(m^{2}K) and the thermal conduction between the iron and cooper is defined by the materials. Based on these conditions, the result for the temperature distribution can be observed in Fig. 3 and Fig. 4.
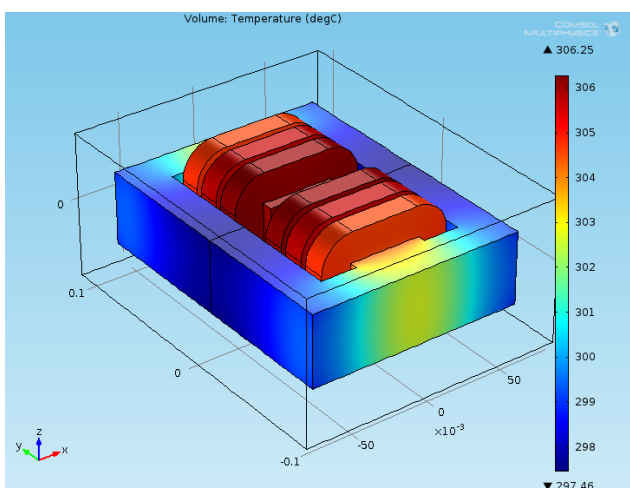

Fig. 3. Temperature Volume plot, 3D view (the axis scale is presented in cm).

The heating effect reaches an equilibrium temperature of 302 K. The hottest parts correspond to the coils and the sample site area, with lower temperatures in the borders of the electromagnet. Such differences are not significant

given the high conductivity of the iron. The simulation shows the expected effects and confirm the need of a cooling system in order to avoid damages to the equipment.
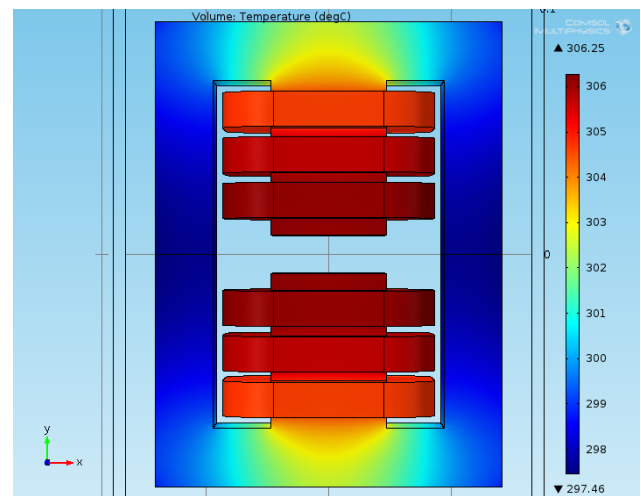

Fig. 4. Temperature Volume plot, top view.

3. Cooling of the electromagnet

It is infeasible to operate the fast field cycling measurements for extended periods of time without a proper cooling system.

An air cooling flow will be applied to the simulation so one may understand and determine the flow requirements to keep the system between a safe temperature range. Given the geometry of the problem it is of interest that the air performs a vertical path so the air flows through the center of the geometry and the surface of the coils where the heat is generated.

In the simulation, it is considered the cooling due to: "Laminar Flow" and "Heat Transfer in Solids". In the Laminar Flow the domain selected is the surrounding air box around the electromagnet and two approaches are defined. The first allows for the free exit of the flow and is defined as the top surface of the air box, while the last represents the cold air flow input that will cool the system, and is defined as the bottom surface of the box. A vertical flow is ensured by these definitions.

The second approach, "Heat transfer in Solids", automatically considers the heat transfer from the coils to the iron electromagnet. A heat transfer rate is calculated depending on the flow instead of the "Convective Cooling" in the Joule Heating which requires a defined fixed heat transfer.

The last and important consideration is the "Mesh". Given the air flow and the sharp edges of the geometry high gradients in velocity fields, and pressure are expected.

This defines the physics of the cooling problem, but a few observations should be noted:

- It is desirable that the flow performs a vertical path, but this does not mean the flow begins it path vertically. It is possible that an horizontal inlet flow is used, and the flow is forced to perform a vertical path. Since the cooling system is not yet defined, an approximation is required for the air path. A total vertical path is suitable given that the air will indeed flow through the inner geometry.

- In the real problem the flow will not assume a laminar flow, but a quite turbulent one given the geometry and the changes the orientation of the flow. Turbulent flow is extremely expensive in terms of computational power, and would not be feasible to simulate given the available computing power of the simulation machine.

Laminar flow provides heat transfer only through conduction because in laminar flow the air is flowing in sheets with little mixing between them. The layer of air that touches the geometry is heated. That layer also does not mix with the other layers of air above it. The heat can only be transferred from one layer to the next by contact (conduction). The turbulent flow has no sheets. This means that more fresh cold gas will contact the surface resulting in a faster heat transfer rate due to a larger average temperature difference between the geometry and air. Given this the laminar flow consideration leads to an over estimative of the required flow, which is desirable in order to allow for several hours of NMR measurements. The "Inlet" and "open boundary" are an exaggeration in terms of the available area since a compact equipment is desired - most likely the flow will both enter and exit by considerable smaller areas. The exaggeration of the inlet area is not a considerable effect since the majority of the air is forced through the middle of the geometry and the smaller the inlet area the more turbulent will be the flow, leading to improved heat transfer to the air. Finally, the exaggeration in the outlet area isn't considered significant since the flow has already gone through electromagnet and performed its cooling effect.

In order to evaluate the air flow cooling effect different flow rates are computed. The software allows for parametric swept of variables and the considered values of the flow rate are : 57.6; 80; 92; 108; 158 and 170 m^3/h. This was obtained after research and evaluation of different available fans in the market that could be implemented in this case. The defined problem for the cooling effect can be summed up to: The electromagnet geometry with six coupled coils, each dissipating a total of 14 W at an initial temperature of 20 ℃. An air laminar flow is immediately forced through the bottom of the electromagnet (in an area slightly bigger than the electromagnet's plane area) and leaves through the top (equal area of the inlet) cooling the geometry. The inlet forces air at 20 ° C and has a defined flow rate (m^3/s).

The results of the computation are 3D plots of three physical quantities: pressure, temperature and air flow velocity. The direction of the flow can be evaluated by the velocity plots.
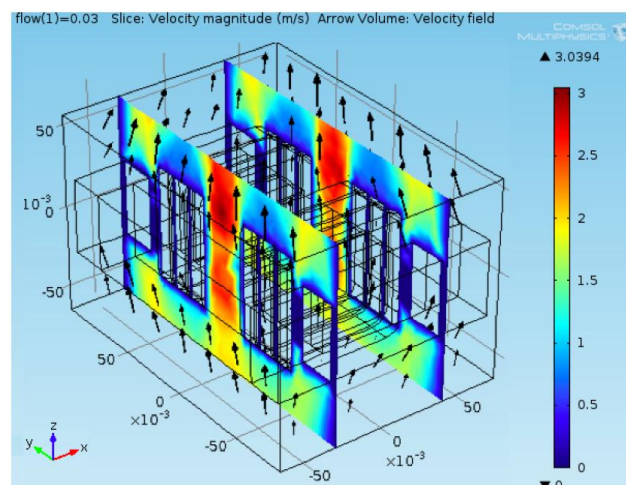

Fig. 5. "Arrow Volume" plot and two "Slice" plots.

The axis scale is presented in m. The black arrows represent the air path, which flows from bottom to top through the geometry (Fig. 5). The "Slice" plots show a high velocity in the middle of the geometry (sample site). In the lateral view of a single centered "Slice" plot allows better observation of the flow velocity (Fig. 6). The flow assumes the highest velocity in the exit at the center and limits of the geometry. The cooling effects occurs mainly in the bottom surface of the coils and lateral surfaces of the outer coils since higher velocity implies enhanced heat transfer. Very low cooling occurs in the inner surfaces of the coils. An increase in distance separating the coils would favor the air cooling.
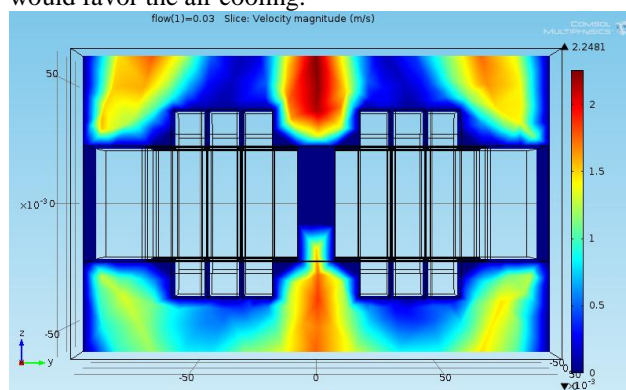

Fig. 6. Geometry centered "Slice" plot, side view.

The temperature data proves that an effective cooling occurs with the air flow method. For a flow rate of 0:03 m^3/s the maximum temperature in the equilibrium corresponds to 46 ℃ and a minimum of 32 ℃ in the electromagnet.
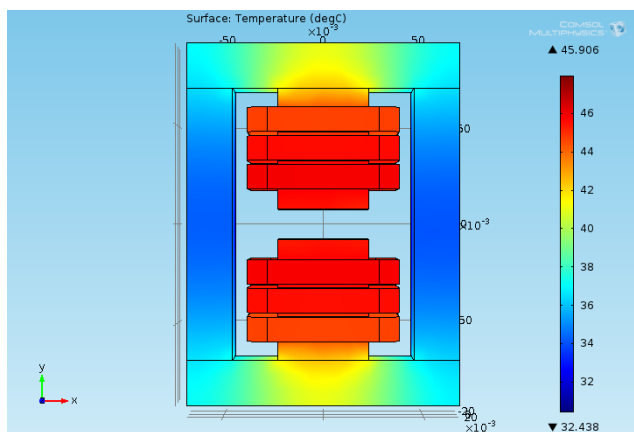
Fig. 7. Temperature "Surface" plot. The axis scale is presented in m.

The highest temperature occurs in the middle of the electromagnet where the coils are placed. A relative colder area is observed in the outer edges without being a significant gradient, proving the high thermal conductivity of the electromagnet. This definitely is an important cooling factor since it spreads out the heat increasing the total transferred energy to the air by increasing the contact area where a temperature gradient exists between electromagnet - air. Such temperatures are acceptable in the perspective that no damage is inflicted to the system when such flow rate is applied for a constant current of 3 A. The temperature plot for a 0.03 m³/s inlet flow rate can be seen in Fig. 7 and Fig. 8. The bottom view of the same plot shows that this side benefits of lower temperature. This is explained by the fact that is the surface that first interacts with the air where it is at its coldest.
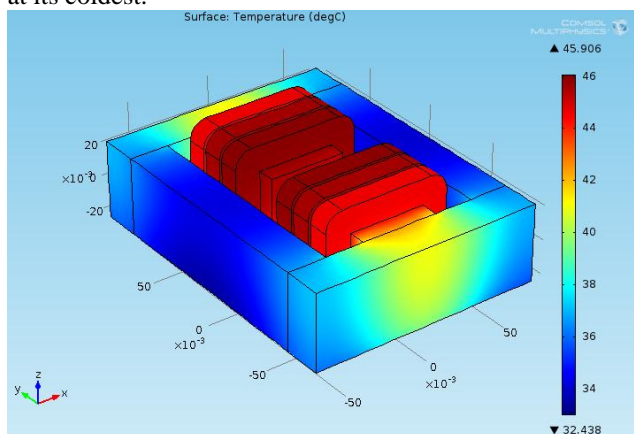

Fig. 8. Temperature "Surface" plot, bottom view. The axis scale is presented in m.

Other flow rates were also computed where the same conclusions are observed but with different equilibrium temperatures. The equilibrium temperatures for different flow rates are compiled in Table I.

Table I. Maximum (Max. T.) and minimum (Min. T.) equilibrium temperature in the electromagnet for a given flow rate.

Flow [m³/s]	Flow [m³/h]	Max. T. [ºC]	Min. T. [ºC]
0.016	57.6	64.2	49.9
0.022	80	53.4	39.4
0.026	92	49.3	35.6
0.03	108	45.9	32.4
0.044	158	38.9	26.6
0.047	170	37.9	25.9

The last set of plots correspond to the Pressure. Although this is not a crucial parameter to consider since all the system will be constituted of solid materials that are not significantly affected by pressure gradients it can be seen as a verification step of the correct definition of the problem. On one hand a higher pressure is expected in the bottom where lower velocities occurs on the other hand lower pressure for the top where the air assumes its higher velocity. This is confirmed by the "Contour line" plot of Fig. 9.
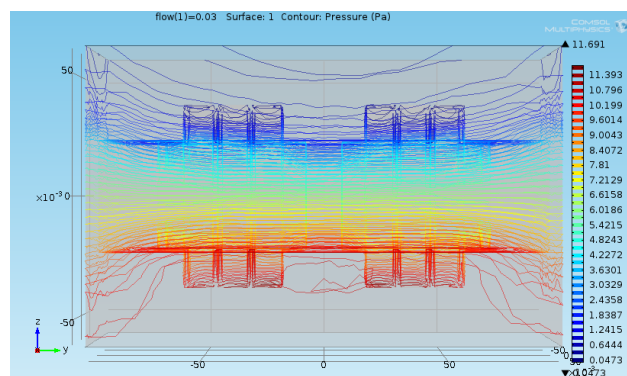

Fig. 9: Pressure "Contour line" plot, side view.

4. Conclusion

For a FFC NMR magnet operating within the magnetic field range of 0 and 0:33 T, the thermal effects and cooling requirements were evaluated allowing for the projection of feasible systems. The computational simulation allowed to estimate air flow rates for safe measurements over extended periods of time. The sample heating system was projected and some components acquired and defined, which guarantees NMR resonance conditions.
The advantages of the developed FFC magnet relatively to the generality of magnets are: reduced electromagnet's volume and weight, low power consumption, high homogeneity prole, feasible and low power cooling system. [19]

Acknowledgement

References

[1] M. Levitt, "Spin Dynamics: Basics of Nuclear Magnetic Resonance", Wiley, 2001.

[2] A. Abragam, "The Principles of Nuclear Magnetism", Oxford University Press, London, 1978.

[3] F. Noack, "NMR Field-Cycling Spectroscopy: Principles and Applications", Prog. NMR Spectrosc., 1986, 18, pp. 171-276.

[4] R. Kimmich and E. Anoardo, "Field-Cycling NMR relaxometry", Progress in NMR Spectroscopy, 2004, 44, pp. 257-320.

[5] E. Anoardo, G. Galli, G. Ferrante, "Fast-Field-Cycling NMR: Applications and Instrumentation", Applied Magnetic Resonance, 2001, 20, (3), pp. 365-404.

[6] R. Seitter, R. Kimmich, "Magnetic Resonance: Relaxometers", in Encyclopedia of Spectroscopy and Spectrometry (Academic Press, London, 1999), pp. 2000-2008.

[7] D. M. Sousa, G. D. Marques, J. Cascais, J. Sebastião, "Desktop Fast-Field Cycling Nuclear Magnetic Resonance Relaxometer", Solid State Nuclear Magnetic Resonance, 2010, 38 (1), pp. 36-43.

[8] D. M. Sousa, G. D. Marques, P. Sebastiao, and A. Ribeiro, "New isolated gate bipolar transistor two-quadrant chopper power supply for a fast field cycling NMR spectrometer", Review of Scientific Instruments, 2003, 74 (3), 4521-4528.

[9] A. Roque, "Espectrómetro de RMN de CCR com utilização de supercondutores no magneto" PhD thesis, Instituto Superior Tecnico, Universidade de Lisboa, 2014.

[10] M. Sciandrone et al., "Compact low field magnetic resonance imaging magnet: Design and optimization", Review of Scientific Instruments, VOL. 71, no. 3, March 2000.

[11] A. E. Umenei et al., "Models for Extrapolation of Magnetization Data on Magnetic Cores to High Fields", IEEE Transactions on Magnetics, VOL. 47, No. 12, December 2011.

[12] S. Hahn et al., "Bulk and Plate Annulus Stacks for Compact NMR Magnets, Trapped Field Characteristics and Active Shimming Performance", IEEE Transactions on Applied Superconductivity, VOL. 23, NO. 3, June 2013.

[13] A. Roque, S. Ramos, J. Barão, V. M. Machado, D. M. Sousa, E. Margato, J. Maia, "Simulation of the Magnetic Induction Vector of a Magnetic Core to be used in FFC NMR Relaxometry", J. Supercond. Nov. Mag., Vol. 26, Issue 1, Page 133-140, 2013.

[14] C. W. T. McLyman, "Tranformer and Inductor Design Hanbook", Second Edition, Marcel Dekker, 1988.

[15] A. Roque, D. M. Sousa, E. Margato, J. Maia, G. Marques, "Characterization of the Fringing Window of a Magnetic Core", Internation Conference on Computer as a Tool (EUROCON 2011), Lisboa, 2011.

[16] J. Fletcher, B. Williams and M. Mahmoud, "Air gap flux fringing reduction in inductors using open-circuit copper screens", IEE Proc.-Electr. Power Appl., Vol. 152, no. 4, pp. 990-996, July 2005.

[17] R. J. Weggel and C. F. Weggel, "High-Homogeneity NMR and MRI Magnets With Minimized Fringe Field", IEEE Transactions on Applied Superconductivity, Vol 24, no. 3, June 2014.

[18] A. Roque, D. M. Sousa, E. Margato, V. M. Machado, P. J. Sebastião and G. D. Marques, "Magnetic Flux Density Distribution in the Air Gap of a Ferromagnetic Core With Superconducting Blocks: Three-Dimensional Analysis and Experimental NMR Results", in *IEEE Transactions on Applied Superconductivity*, vol. 25, no. 6, pp. 1-9, Dec. 2015.

[19] P. Videira, P. Sebastião, A. Roque, D. M. Sousa, E. Margato, "Fast-Field Cycling Nuclear Magnetic Resonance relaxometer's electromagnet with optimized homogeneity and reduced volume" International Conference on Renewable Energies and Power Quality (ICREPQ'19), 2019.